JOURNAL OF GUIDANCE, CONTROL, AND DYNAMICS
Vol. 19, No. 6, November–December 1996

Mercury Sun-Synchronous Polar Orbits Using Solar Sail Propulsion

Manfred E. Leipold*
German Aerospace Research Establishment, Cologne 51147, Germany
and
Otto Wagner†
Technical University of Munich, Munich 80290, Germany

As the oblateness of Mercury is nearly zero, an orbit about the planet will not precess without propulsive acceleration but instead will remain inertial. This causes the spacecraft to encounter a very severe thermal environment when passing near the subsolar point of Mercury's hot surface. An innovative concept applying solar sail propulsion in Mercury orbit is described where the low-thrust propulsion capability is used to realize a sun-synchronous orbit about the planet. The spacecraft is able to continuously move near the terminator, which substantially reduces the thermal hazards and also allows suitable conditions for remote sensing. Circular as well as eccentric polar orbits were investigated concerning their potential to realize the required rotation rate of the line of nodes. For the elliptical orbits, the periapsis is located above Mercury's north pole. Because of Mercury's 3:2 spin-orbit coupling, relative motion between the spacecraft's orbital plane and Mercury will result, allowing complete coverage of the planet's surface. The variation of the solar flux over a Mercury year caused by the high orbit eccentricity of the planet around the sun is also considered. Alternatively to solar sailing, chemical and electric propulsion are analyzed concerning the applicability for orbit precession at Mercury.

Introduction

SOLAR sails are advanced spacecraft concepts using the solar radiation pressure on large reflecting sails for low-thrust propulsion. Solar sailing has been proposed and investigated already in the past for its application as a propulsion technique for space transportation to reach Mercury.[1–3] In most studies the sail is only used for the interplanetary transfer and is jettisoned upon Mercury encounter. However, sail vehicles are very effective in the vicinity of Mercury because of the increased solar radiation pressure. Therefore, solar sailing may also be used for planetocentric trajectories about Mercury.[3]

Orbit design about Mercury requires a tradeoff between observation conditions and spacecraft thermal design, especially for an imaging mission. In contrast to a magnetospheric mission where highly elliptical orbits are desired, relatively low altitudes would be required to obtain high ground resolution for imaging, while global coverage should still be achieved. On the other side, constraints such as the harsh thermal environment, affecting spacecraft survivability and lifetime, restrict the choice of the orbit: Besides a maximum of 10.6 solar constants (SC) direct solar flux at Mercury perihelion, the spacecraft may encounter as much as 8 SC in a low altitude above the subsolar point, caused by the heat reflected and reradiated from the sunlit surface. Previous studies have shown that thermal survival in a low circular Mercury orbit seems not possible applying conventional thermal control techniques and standard spacecraft configurations.[4]

Once in orbit about Mercury, the high acceleration potential of a sailcraft and the low gravitational field of the planet allow the use of solar sailing to change the orbit geometry and orientation. Because of the "unlimited propellant" of solar sails, essentially any orbit about Mercury may be achieved. Considering the thermal constraints mentioned earlier, as well as the solar sail propulsion capabilities, orbit geometries and navigation concepts have been analyzed that allow the rotation of the line of nodes corresponding to the sun-synchronous condition. This allows the spacecraft to continuously move near Mercury's terminator, avoiding passages of the subsolar point. This orbit design has several advantages.

1) The thermal loading as a result of reflection and reradiation from Mercury's surface presents no major additional threat to the spacecraft. Passage of Mercury's shadow is eliminated, thus avoiding severe temperature shocks.

2) The low sun angles near the terminator on the sunlit side—when providing a small offset of the orbital plane from the terminator—will allow high topographic discrimination, which is more difficult for high sun angles. Moreover, this orbit design results in basically constant illumination conditions for imaging at all longitudes, allowing direct comparison of measurements.

3) Since Mercury's rotation period (58.6 days) and orbital period (88 days) are in a 3:2 resonance, this orbit design will allow complete coverage of Mercury's surface. Because of this 3:2 spin-orbit coupling, relative motion between the orbital plane and the planet's surface occurs, allowing passage of all longitudes.

Orbit Design Analysis

Considering Mercury's orbital period around the sun, a sun-synchronous orbit about the planet would correspond to an average rate of change of the longitude of the ascending node Ω of

$$\bar{\dot{\Omega}} = \frac{2\pi}{87.97 \times 24 \times 3600\,\mathrm{s}} = 8.27 \times 10^{-7}\,\frac{\mathrm{rad}}{\mathrm{s}} \tag{1}$$

Actually, because of Mercury's high orbit eccentricity of about 0.2, the required rotation rate of the line of nodes varies over a Mercury year. The actual values may be calculated using the relation for the rate of change of the true anomaly ν_M of Mercury around the sun, which also corresponds to the progression of the terminator:

$$\dot{\Omega} = \frac{\mathrm{d}\nu_M}{\mathrm{d}t} = \frac{h_M}{R^2}\left[\frac{\mathrm{rad}}{\mathrm{s}}\right] \tag{2}$$

where h_M is Mercury's specific angular momentum with respect to the sun (2.713×10^{15} m^3/s^2) and R is the distance from the sun. Therefore, the required rotation rate for a sun-synchronous orbit varies between 1.28×10^{-6} rad/s during perihelion passage and 5.57×10^{-7} rad/s at Mercury aphelion.

Received April 17, 1995; revision received June 24, 1996; accepted for publication June 24, 1996.

*Research Scientist, Space Systems Analysis Division. Member AIAA.
†Professor, Department of Flight Mechanics and Flight Control.

The orbit geometry, orientation, and required sail attitude with respect to the sun can be derived by analyzing Lagrange's planetary equation for the perturbed orbital motion,[5] where

$$\dot{\Omega} = \frac{r f_n \sin(\omega + \nu)}{h \sin i} \tag{3}$$

with

$$h^2 = \mu_M a(1 - e^2), \qquad (\omega + \nu) = u \tag{4}$$

where r is the orbital radius, f_n is the component of the perturbing acceleration f normal to the osculating orbital plane, h is the specific angular momentum of the spacecraft, and i is the orbit inclination with respect to the equator. The gravitational parameter μ_M of Mercury is 2.2032×10^{13} m^3/s^2, a is the semimajor axis, and e is the orbit eccentricity. The argument of periapsis is denoted by ω, and ν is the true anomaly, while the parameter u is called the argument of latitude.

The acceleration as a result of solar pressure, assumed to be always directed towards the unit vector $\boldsymbol{e}_n$ normal to the sail surface (defining the sail attitude), can be expressed by

$$\boldsymbol{f}_n = 2\eta(\mathrm{SC}/c)(1/R)^2(1/\sigma)\cos^2\beta \boldsymbol{e}_n \tag{5}$$

The parameter η, the sail efficiency, includes nonperfect reflection and warping effects of the sail, where a value of 0.89 is assumed.[6] SC is the solar constant at 1 AU (1358 W/m^2), the solar distance R is expressed in astronomical units, and c is the speed of light ($c = 2.9979 \times 10^8$ m/s). The angle β is the sun incidence angle (between the sunlight direction and the sail normal). The acceleration potential of the sailcraft is given in terms of the sail loading σ, which is defined as the ratio of the total spacecraft mass m_{SC} and the sail area A:

$$\sigma = m_{\mathrm{SC}}/A \tag{6}$$

The maximum acceleration a sailcraft can experience at 1 AU solar distance is called the characteristic acceleration a_c. Using Eq. (5), a_c can be expressed by

$$a_c = 2\eta\frac{\mathrm{SC}}{c\sigma} \approx \frac{8.1 \times 10^{-6}[\mathrm{kg/(m \cdot s^2)}]}{\sigma} \tag{7}$$

This parameter best characterizes the performance of a solar sail spacecraft. Values between 0.25 and 1 mm/s^2 are used here in a parameter analysis concerning the influence on the orbit geometry. Since at Mercury's perihelion distance the solar flux is increased to about 10.6 SC, a sailcraft with a characteristic acceleration a_c of 0.25 mm/s^2 corresponding to a sail loading σ of about 32 g/m^2 would be able to provide a propulsive acceleration of 2.65 mm/s^2. For a spacecraft with a total mass of 250 kg this would transfer to a thrust level of about 660 mN. However, because of extended flight times of several years for the interplanetary transfer from Earth (about 2.5–3 years for $a_c = 0.25$ mm/s^2)[3] and for spiraling in Earth-moon-space to escape, degradation of the sail because of particle impact and environmental effects will occur. This variation is not considered in the present analysis, and the characteristic acceleration is assumed to be constant.

As seen in Eq. (3), the component of the acceleration as a result of solar pressure perpendicular to the plane of the osculating orbit f_n is used to rotate the line of nodes to achieve the prograde rotation rate required for a sun-synchronous orbit. Near-circular and elliptical orbits were investigated concerning their potential to achieve the required rotation rate. Circular orbits basically allow to rotate the line of nodes. The analysis has shown, however, that turn maneuvers of the sail twice each orbit are required. During the thrust phase for half an orbit, the sail surface is exposed to the sun, providing the acceleration normal to the osculating orbital plane. During the rest of the orbit, the sail is turned edgewise to the sun, avoiding a retrograde effect on the rotation of the line of nodes corresponding to a sign change of $\sin(\omega + \nu)$. The radius for this orbit and this sail strategy has been determined to about 51,000 km.[3] This orbit, however, is subject to large inclination changes as a result of solar sail propulsion and gravitational perturbations of the sun. The rate of change of inclination can be determined with Lagrange's planetary equation[5]

$$\dot{i} = \frac{r f_n \cos(\omega + \nu)}{h} \tag{8}$$

The maximum rate of change for a circular orbit of 51,000-km radius and a solar sail acceleration f_n of 2.65 mm/s^2 at Mercury perihelion can be determined to 4.02×10^{-6} rad/s. Consequently, half a revolution can result in an inclination change of more than 35 deg.

Since the circular orbit proved to be too high in altitude to be suitable for remote sensing of Mercury's surface and is also highly unstable, eccentric orbits were investigated in more detail. Integration of the perturbing acceleration over a period $(t_1 - t_0)$, based on Eq. (3), results in a change of the longitude of the ascending node of

$$\Delta\Omega|_{t_0}^{t_1} = \frac{f_n}{h \sin i}\int_{t_0}^{t_1} r \sin(\omega + \nu)\,\mathrm{d}t \tag{9}$$

where average values for the spacecraft's specific angular momentum h, inclination, semimajor axis, eccentricity, and argument of periapsis are assumed to be constant. This was shown to hold, since only small short-period variations of the inclination and long-period variations of the argument of periapsis occur for low-altitude elliptical orbits. As, moreover, the sail orientation with respect to the sun remains constant over one orbital revolution (i.e., $\beta = 0$ deg for orbits along the terminator to provide maximum acceleration normal to the orbital plane), f_n is also constant. Substitution of

$$\mathrm{d}t = (r^2/h)\mathrm{d}\nu \tag{10}$$

corresponding to Kepler's second law and integration over one orbital revolution yield

$$\Delta\Omega|_{\omega+\nu=0}^{\omega+\nu=2\pi} = \frac{f_n}{h^2 \sin i}\int_{\omega+\nu=0}^{2\pi} r^3 \sin(\omega + \nu)\,\mathrm{d}\nu \tag{11}$$

With

$$r = \frac{a(1 - e^2)}{1 + e\cos\nu} \tag{12}$$

Eq. (11) can be rewritten as

$$\Delta\Omega|_{\omega+\nu=0}^{\omega+\nu=2\pi} = \frac{f_n[a(1 - e^2)]^3}{h^2 \sin i}\int_{\omega+\nu=0}^{2\pi} \frac{\sin(\omega + \nu)\,\mathrm{d}\nu}{(1 + e\cos\nu)^3} \tag{13}$$

The precession rate of the nodal line can then be calculated using the orbital period T and Eq. (4)

$$\dot{\Omega} = \frac{\Delta\Omega|_{\omega+\nu=0}^{\omega+\nu=2\pi}}{T} = \frac{\Delta\Omega|_{\omega+\nu=0}^{\omega+\nu=2\pi}}{2\pi\sqrt{a^3/\mu_M}} \tag{14}$$

$$\dot{\Omega} = \frac{\sqrt{a} f_n(1 - e^2)^2}{2\pi\sqrt{\mu_M}\sin i}\int_{\omega+\nu=0}^{2\pi} \frac{\sin(\omega + \nu)\,\mathrm{d}\nu}{(1 + e\cos\nu)^3} \tag{15}$$

By placing the periapsis location above the north pole ($\omega = 90$ deg), the maximum effect of the perturbation will occur in the vicinity of the apoapsis, where the orbital radius r and $\sin(\omega + \nu)$ have an extremal point, and the spacecraft spends an extended time. Given a certain periapsis altitude, the proper apoapsis radius to realize the required rotation rate of the line of nodes remains to be determined. Using

$$a = \frac{r_P + r_A}{2} \tag{16a}$$

$$e = 1 - (r_P/a) \tag{16b}$$

where r_P is the periapsis radius and r_A the apoapsis radius, respectively, the proper apoapsis altitude for a given acceleration f_n normal

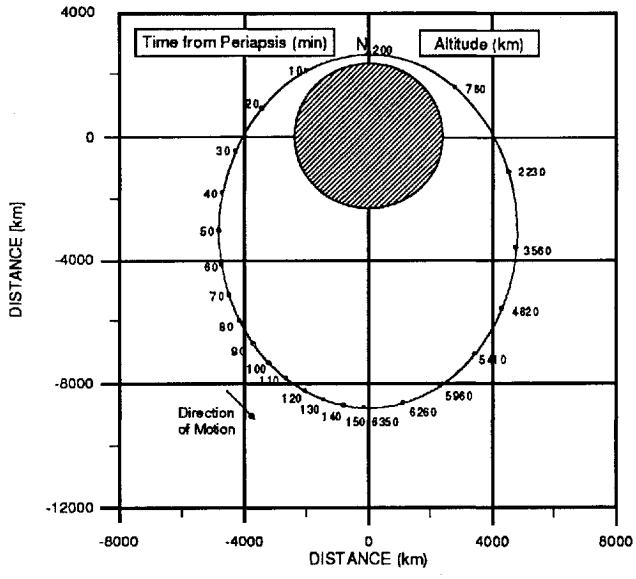

Fig. 1 Geometry for elliptical orbit ($a_c = 0.25$ mm/s^2) along Mercury's terminator (view from the sun).

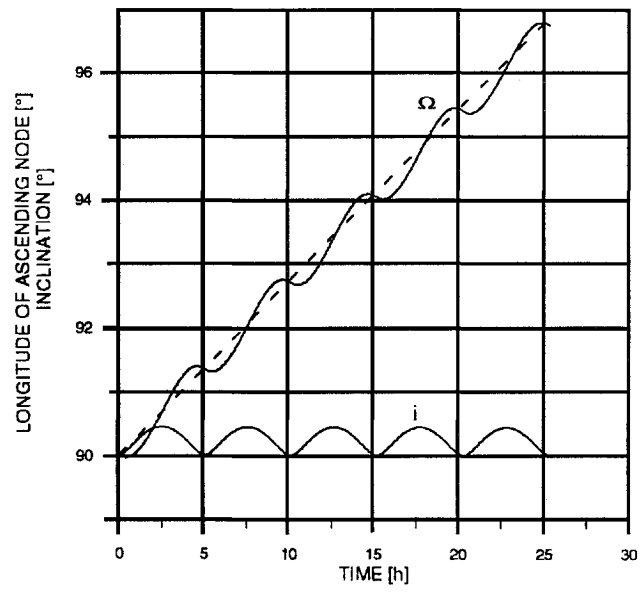

Fig. 2 Progression of nodal line and inclination changes for five consecutive orbits ($a_c = 0.25$ mm/s^2) at Mercury perihelion.

to the plane of the osculating orbit can be determined by numerical integration of Eq. (15).

For a solar sail spacecraft with $a_c = 0.25$ mm/s^2, where for the nominal orbit the periapsis is set to 200 km above Mercury's north pole and the spacecraft moves along Mercury's terminator, the apoapsis altitude was determined to approximately 6350 km. The orbit eccentricity is 0.538, and the orbital period for this orbit is about 5.08 h. This orbit as seen from the direction of the sun, including time from periapsis passage and altitude, is shown in Fig. 1.

In this orbit design the sail is oriented to provide maximum acceleration perpendicular to the orbital plane during the whole orbital revolution. Therefore, no turn maneuvers of the sail are required. This results in a small retrograde rotation of the line of nodes when the spacecraft is north of the equator where $0 \leq u \leq \pi$, but this contribution is dominated by the orbit phase south of the equator, which provides the required prograde rotation.

To verify the results, trajectories are generated numerically using a variable order variable step size Adams–Bashforth–Moulton method including interpolation for the output. The equations of motion of the solar sail spacecraft are expressed in a system of six first-order differential equations, here written in vector form:

$$\dot{\boldsymbol{r}} = \boldsymbol{v} \tag{17}$$

$$\dot{\boldsymbol{v}} = -\mu_M(\boldsymbol{r}/r^3) + 2\eta(\mathrm{SC}/c)(1/R)^2(1/\sigma)\cos^2\beta \boldsymbol{e}_n \tag{18}$$

The Cartesian position and velocity components are converted to classical orbital elements for additional output. Figure 2 shows the progression of the line of nodes and periodic variation of the inclination based on the orbit geometry described earlier, with the assumptions of a characteristic acceleration of $a_c = 0.25$ mm/s^2 and 10.6 SC of solar flux at Mercury perihelion ($f_n = 2.65$ mm/s^2). The dashed line of Fig. 2 indicates the average change of the longitude of the ascending node, which corresponds to the required rate of change of 1.28×10^{-6} rad/s during perihelion passage.

At the same time the inclination exhibits a weak short-period variation of about ± 0.25 deg. The corresponding maximum rate of change of inclination based on Eq. (8) can be determined to about 3.6×10^{-8} rad/s, which is roughly two orders of magnitude smaller than for the high-altitude circular orbit described earlier. The argument of periapsis shows a long-period variation with an amplitude of approximately ± 0.4 deg (not shown).

Alternatively, considering a retrograde orbit, the periapsis location would be above the south pole, where the orbit geometry, however, is the same as for a prograde orbit with periapsis above the north pole as shown in Fig. 1. In a more advanced scenario it is also conceivable that two solar sail spacecraft are in orbit about Mercury,

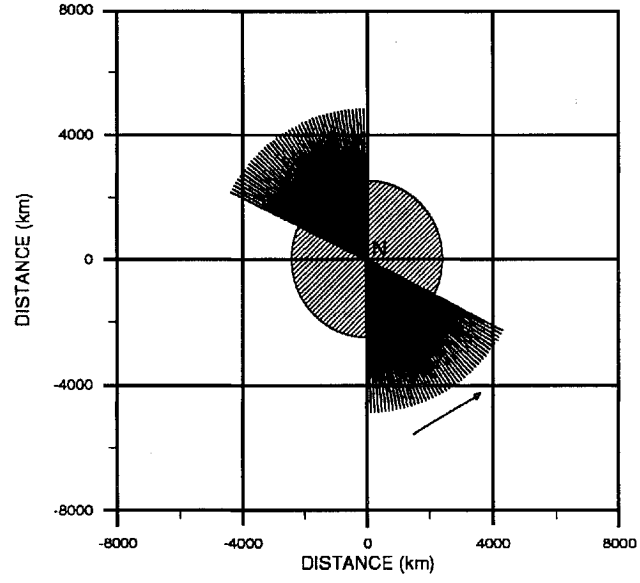

Fig. 3 Progression of the orbital plane about Mercury at perihelion ($a_c = 0.25$ mm/s^2) (view from above the north pole for 45 revolutions).

one moving prograde with periapsis above the north pole, and one moving retrograde with periapsis above the south pole. This would allow for very high resolution imaging for both the northern and the southern hemisphere.

Numerical trajectory simulation has furthermore been performed to show the progression of the orbit plane about Mercury. Figure 3 depicts the sun-synchronous orbit simulated for $a_c = 0.25$ mm/s^2 and 45 revolutions as seen from above the north pole. As for the analysis shown in Fig. 2, in this calculation it was assumed that Mercury is at its perihelion so that about 10.6 SC of solar flux are available to propel the sailcraft.

The varying rotation rate $\dot{\Omega}$ of the line of nodes during one Mercury year as a result of the planet's high orbit eccentricity around the sun seems to require an adjustment of the orbit geometry. However, because both the required precession of the orbit and solar sail propulsion show a $1/R^2$ dependency [see Eqs. (2) and (5)], the rotation of the line of nodes is adjusted automatically over a Mercury year, and the orbit can be maintained. Solar sails, therefore, possess a unique property for the realization of a sun-synchronous orbit about Mercury.

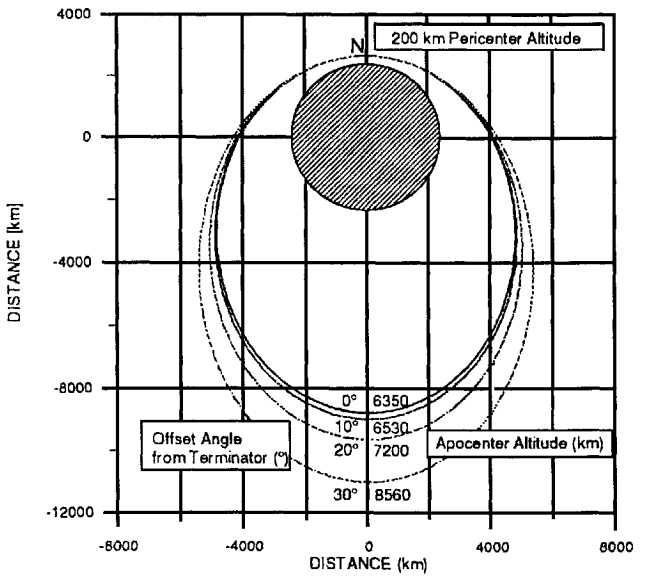

Fig. 4 Orbit geometry for different offset angles from the terminator ($a_c = 0.25$ mm/s^2).

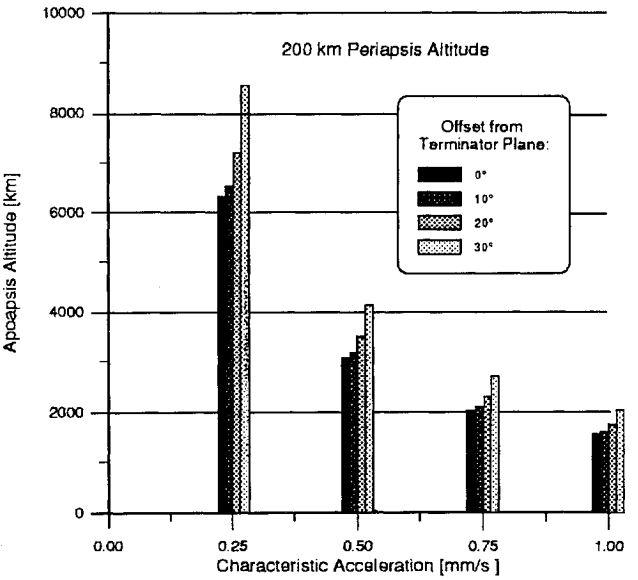

Fig. 5 Influence of characteristic acceleration and offset from the terminator on apoapsis altitude.

Variation of the Sun Phase Angle

For an imaging mission, moving directly along Mercury's terminator may pose difficulties for visual mapping because of very long shadow lengths, and topographic discrimination could be difficult. Consequently, an analysis was carried out to investigate the possibility to provide an offset from the terminator. Here the orbit is rotated around the line of apsides by an angle α from its alignment with the terminator plane by choosing the appropriate longitude of ascending node, so that the orbit nodal line is not perpendicular to the sun direction any more.

This causes the spacecraft on one subarc of the orbit to pass over the sunlit side, whereas the groundtrack of the other subarc is on the night side of the surface. The spacecraft, however, remains still in permanent sunlight as long as α remains below about 50 deg. This offset has an impact on the orbit geometry: higher apoapsis altitudes are required to adjust the decreased propulsive acceleration perpendicular to the plane of the osculating orbit. The orbit geometry for different offset angles α from the terminator plane is shown in Fig. 4 for a sailcraft with $a_c = 0.25$ mm/s^2, determined by solving Eq. (15) together with Eq. (16) and then integrating numerically.

To allow direct comparison of the orbit geometry, each trajectory in Fig. 4 is shown as seen from a direction perpendicular to the orbital plane despite different orientations in inertial space (rotation around the line of apsides not shown). As in the case of the orbit aligned with the terminator, the sail attitude is chosen so that the sail normal is perpendicular to the orbital planes with offset from the terminator.

Because of Mercury's 3:2 spin-orbit coupling, the spacecraft passes over each longitude within one Mercury year, allowing complete coverage of Mercury's surface. Since, however, because of the offset from the terminator part of the groundtrack is on Mercury's night side, the spacecraft is expected to remain in this orbit for two Mercury years (about 176 days) during which Mercury rotates once under this sun-synchronous orbit. This allows complete coverage of all longitudes on the sunlit side. High latitudes on the northern hemisphere would be imaged from a low altitude allowing high-resolution imaging, including search for indicated polar ice deposits, whereas the southern hemisphere could be covered with less ground resolution. Consecutive orbits, where the groundtracks will have a longitudinal difference of only about 40 km at the equator, will provide longitudinal overlap for imaging. Furthermore, this orbit allows passage of Mercury's magnetosphere (tail diameter about 6 planetary radii ≈14,700 km), where the spacecraft crosses the magnetopause near apoapsis.

Variation of the Characteristic Acceleration

The analysis for elliptical orbits presented earlier is based on a sailcraft characteristic acceleration of 0.25 mm/s^2. More advanced solar sails with even higher propulsive capability, applying more advanced lightweight structures and materials, may be considered. Therefore, the characteristic acceleration was varied in this analysis to determine the orbit geometry, where the periapsis was set at a 200-km altitude above Mercury's north pole. Figure 5 shows the results for apoapsis altitude for the variation of characteristic acceleration (0.25, 0.50, 0.75, and 1.00 mm/s^2) for different offset angles from the terminator as determined by numerical analysis.

If the characteristic acceleration is increased to 0.50 mm/s^2, the apoapsis altitude can be lowered to about 3080 km for small offsets from the terminator. A further increase of a_c allows a further decrease in apoapsis altitude. Assuming a rather advanced solar sail with $a_c = 1$ mm/s^2, a 200-km periapsis, 1570-km apoapsis altitude sun-synchronous orbit along the terminator could be realized. Furthermore, it can be seen that the impact of the offset from the terminator on apoapsis altitude is reduced for high accelerations.

The overall high performance of solar sails in Mercury orbit may be stressed by calculating the order of magnitude of the Δv provided by solar sail propulsion during one Mercury year. Considering an even moderate value for the characteristic acceleration of 0.25 mm/s^2, the average acceleration at mean Mercury solar distance (semimajor axis of 0.387 AU) is 1.67 mm/s^2. During 88 days such a solar sail spacecraft will provide a low-thrust Δv on the order of approximately

$$\Delta v \approx 1.67 \times 10^{-3}\text{m/s}^2 \times 88 \times 86{,}400\,\text{s} \approx 12.7\,\text{km/s}$$

In this case the propulsive capability is used for orbit precession, not for changing the orbital energy. The high Δv, however, indicates that solar sails could be very effective for both orbit capture and planetary escape at Mercury.

Application of Chemical Propulsion for Orbit Precession

Alternatively to solar sailing, application of chemical propulsion may be considered to rotate the line of nodes. As Mercury's oblateness is essentially zero, and the nodal line of a polar orbit is not influenced by the J_2 effect, impulsive maneuvers have to be applied to realize the required orbit precession for a sun-synchronous orbit.

The Δv requirement applied normal to the osculating orbit plane can be calculated with

$$\Delta v_n = \Delta\Omega \frac{\mu_M \sqrt{1-e^2}\sin i}{nar\sin(\omega+\nu)} \tag{19}$$

with

$$n = \sqrt{\mu_M / a^3} = 2\pi/T \tag{20}$$

Table 1 Propellant requirement for orbit precession using chemical propulsion

m_{SC}, kg	300	500	1000
m_P, kg: $\Delta\Omega = 2.05$ deg	1.8	3.1	6.2
m_P, kg: $\Delta\Omega = 360$ deg	198	330	660

based on Gauss' variational equations,[5] where n expresses the mean motion. The most effective location on the orbit to apply impulsive thrust, therefore, as in the solar sail orbit design, occurs when the magnitude of $\sin(\omega + \nu)$ equals 1, and if the elliptical orbit is oriented properly, moreover, the orbital radius r is also at maximum (at apoapsis). Equation (19) also indicates that changing the nodal line is not possible when the impulses are applied at the nodes where $\sin(\omega + \nu)$ equals 0.

The reference orbit considered here is a 12-h elliptical orbit with a 200-km periapsis altitude and a 15,000-km apoapsis altitude,[7] which would provide favorable conditions for orbit precession because of the relatively large orbital radius at apoapsis. To realize a 360-deg rotation of the nodal line of a 12-h orbit within 88 days, a shift of about 2.05 deg is required for each apoapsis passage. Considering $\omega = 90$ deg, to realize a 2.05-deg shift of the nodal line, an impulsive Δv_n of about 20.6 m/s is required when applied at apoapsis according to Eqs. (19) and (20). The total Δv requirement over one Mercury year then amounts to 3.6 km/s.

The propellant requirement m_P may then be calculated using

$$m_P = m_{SC}\left[1 - \exp\left(-\frac{\Delta v_n}{I_{sp}g}\right)\right] \tag{21}$$

where m_{SC} is the spacecraft mass in Mercury orbit, I_{sp} is the specific impulse in seconds, and g is the gravity constant of the Earth. Table 1 shows the propellant requirement to provide a precession of the orbit of 2.05 and 360 deg, respectively, for different initial spacecraft masses in Mercury orbit, where a specific impulse of 340 s was assumed for the bipropellant system (e.g., N_2O_4 and MMH).

The propellant requirement for a 360-deg rotation of the line of nodes was determined assuming impulses during each apoapsis passage providing incremental 2.05-deg rotations of the line of nodes and considering the decrease in total spacecraft mass. As can be seen from Table 1, the propellant fraction is 66% of the spacecraft mass in orbit for a 360-deg rotation of the nodal line and will most likely exceed the capability and mass constraints of a conventional spacecraft.

Application of Electric Propulsion for Orbit Precession

Electric propulsion may also be reviewed concerning its applicability to realize a sun-synchronous orbit about Mercury. Similar to the solar sailing mode, varying accelerations normal to the plane of the osculating orbit are required as Mercury progresses around the sun. Taking the eccentric orbit geometry aligned with the terminator as determined for a solar sail with $a_c = 0.25$ mm/s^2, as mentioned earlier accelerations of 1.15 to 2.65 mm/s^2 are required in Mercury orbit to obtain the adequate rotation of the line of nodes. Table 2 shows the thrust level range over one Mercury year necessary for electric thrusters, depending on initial spacecraft mass in Mercury orbit.

Considering ion thrusters currently under development such as the ESA-26 ion thruster with a maximum thrust level of 200 mN (Ref. 8), this thrust level would require four ESA-26 engines for a 300-kg spacecraft. With an individual power input of about 6.2 kW, the total power requirement would amount to a maximum of approximately 25 kW for a thrust level of 800 mN. This would demand a heavy power supply subsystem, which seems very difficult to be accommodated within the limited spacecraft mass budget.

Table 2 Thrust level range requirement using electric thrusters for orbit precession

m_{SC}, kg	300	500	1000
F, N	$0.35 \cdots 0.80$	$0.58 \cdots 1.33$	$1.15 \cdots 2.65$

Conclusions

Solar sails in orbit about Mercury are very effective because of the high solar radiation pressure and the weak gravitational field of the planet. Using this basically unlimited propulsive capability, the orbit orientation in inertial space can be modified to realize a sun-synchronous orbit about Mercury. The thermal hazards can be reduced by avoiding passage of Mercury's hot surface near the subsolar point by aligning the orbital plane with Mercury's terminator. Circular orbits were shown to be too high in altitude for remote sensing of Mercury's surface and are, moreover, subject to large variations in inclination. Eccentric orbits where the periapsis is located above Mercury's north pole seem to be the most suitable since they are stable in inclination and periapsis location. For a Mercury planetology mission the proposed orbit seems quite favorable to conduct surface-related remote sensing. Relatively low altitudes from 200 to 6350 km can be realized, while global coverage is possible because of Mercury's 3:2 spin-orbit coupling. To improve lighting conditions for visual imaging, an offset from the terminator plane may be introduced, slightly increasing apoapsis altitude as a result of loss of propulsive capability as the acceleration normal to the plane of the osculating orbit is decreased. Advanced solar sails may allow the spacecraft to get closer to the planet as the apoapsis altitude can be decreased. Since both the required precession rate of the nodal line and solar sail propulsion have the same inverse square variation with respect to solar distance, the rotation of the orbit is adjusted automatically over a Mercury year, and the orbit geometry can be maintained. Thus solar sails possess a unique property for the realization of a sun-synchronous orbit about Mercury.

Application of chemical or electric ion propulsion for orbit precession about Mercury seems feasible, in theory. However, using chemical propulsion to realize a sun-synchronous orbit requires a substantial amount of propellant mass, which has to be delivered to Mercury orbit. On the other hand, the high thrust level for ion propulsion of several hundred milli-Newtons up to several Newtons depending on the overall spacecraft mass and the associated high power input requirement may be difficult to implement within a limited spacecraft mass. Extending the basic concept, sun-synchronous solar sail orbits could be designed around other celestial bodies primarily in the inner solar system, especially when the associated gravitational field of the target object does not allow sufficient orbit precession, or application of chemical and electric propulsion is not possible because of limited mass or power supply.

References

[1]French, J. R., and Wright, J., "Solar Sail Missions to Mercury," *Journal of the British Interplanetary Society*, Vol. 40, Dec. 1987, pp. 543–550.

[2]Sauer, C., "Optimum Solar Sail Interplanetary Trajectories," AIAA Paper 76-792, Aug. 1976.

[3]Leipold, M., Borg, E., Lingner, S., Pabsch, A., Sachs, R., and Seboldt, W., "Mercury Orbiter with a Solar Sail Spacecraft," *Acta Astronautica*, Vol. 35, Supplement 2, 1995, pp. 635–644.

[4]French, J., Stuart, J. R., and Zeldin, B. I., "New Concepts for Mercury Orbiter Missions," AIAA Paper 78-79, Jan. 1978.

[5]Battin, R. H., *An Introduction to the Mathematics and Methods of Astrodynamics*, AIAA Education Series, AIAA, New York, 1987, pp. 476–490.

[6]Wright, J. L., *Space Sailing*, Gordon and Breach, Philadelphia, PA, 1992, Philadelphia, pp. 55, 56.

[7]Nelson, R. M., Horn, L. J., Weiss, J. R., and Smythe, W. D., "Hermes Global Orbiter—A Discovery Mission in Gestation," *Acta Astronautica*, Vol. 35, Supplement, 1995, pp. 387–395.

[8]Groh, K. H., Fahrenbach, P., and Loeb, H. W., "Tests on the European Primary Radio-Frequency Engine ESA XX," AIAA Paper 94-3391, June 1994.